



Degradation of ibuprofen by a synergistic UV/Fe(III)/Oxone process



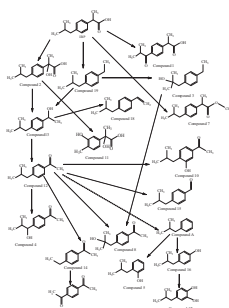
YongFang Rao*, Dan Xue, Huaimin Pan, Jiangtao Feng, Yingjie Li

Department of Environmental Science and Engineering, Xi'an Jiaotong University, Xi'an 710049, China

HIGHLIGHTS

- Degradation of ibuprofen by UV/Fe³⁺/Oxone process is reported.
- Ibuprofen degradation rate depends on pH value and the ratio of [Fe³⁺]:[Oxone]:[IBP].
- The anions Cl[−], SO₄^{2−} and H₂PO₄[−] caused a negative effect on ibuprofen degradation.
- NO₃[−] slightly accelerated ibuprofen degradation.
- Six new intermediates/byproducts were identified.

GRAPHICAL ABSTRACT



ARTICLE INFO

Article history:

Received 4 February 2015

Received in revised form 18 June 2015

Accepted 16 July 2015

Available online 23 July 2015

Keywords:

Ibuprofen
Sulfate radicals
Hydroxyl radicals
Decarboxylation
Hydroxylation

ABSTRACT

In this study, the degradation of a widely used non-steroidal anti-inflammatory drug ibuprofen (IBP) by UV/Fe(III)/Oxone was conducted. IBP decomposition by sole-UV, UV/Fe(III), Fe(III)/Oxone and UV/Oxone processes was also carried out to evaluate the isolated effects contributing to IBP degradation. The influence of pH levels, the concentration of Fe(III) and Oxone, and inorganic anions on the performance of UV/Fe(III)/Oxone process was evaluated. SPME (Solid phase microextraction)/GC/MS were used to identify the intermediates for the first time. Nineteen intermediates/byproducts were detected during IBP degradation, among which six escaped from the detection in previous studies. Based on the analysis of intermediates, possible decay pathways of IBP were proposed accordingly. Decarboxylation and hydroxylation were believed to be major reaction mechanisms involved in IBP degradation by UV/Fe(III)/Oxone process.

© 2015 Elsevier B.V. All rights reserved.

1. Introduction

Pharmaceuticals detected in the environment are identified as emerging pollutants. Due to the increasing consumption, inappropriate disposal and their incomplete elimination in wastewater treatment plants (WWTP), pharmaceuticals have been found ubiquitously in natural waters [1–5]. The majority of these compounds exist in the aquatic environment at trace level and demonstrate relatively low acute toxicity, however, little is known about synergistic effects of pharmaceutical mixtures and the long-term effects of continuous exposure to these compounds and their metabolites [6].

Non-steroidal anti-inflammatory drugs (NSAIDs) are a group of widely used pharmaceuticals that are frequently found in aquatic environment. Ibuprofen (IBP), a typical NSAID, is prescribed against musculature pain and inflammatory rheumatic disorders. It is also used for analgesic and antipyretic purposes. This drug is ranked the 17th place on the list of most prescribed drugs in the United States [7]. The production volume of IBP is estimated to be 15,000 tons per year, which is ranked the third position after aspirin [8]. Industrial and domestic routes were considered as the major contamination pathways for IBP in aquatic environment. Industrial pollution comes from the release of untreated effluents from the pharmaceuticals companies while domestic contamination is due to the excretion by humans after partial metabolism and inappropriate disposal of IBP [9]. Wastewater treatment plants (WWTPs)

* Corresponding author.

E-mail address: yf Rao@mail.xjtu.edu.cn (Y. Rao).

have been found incapable to completely remove IBP via biodegradation [10–12]. Thus, IBP has been frequently and extensively detected in surface waters and even in drinking water due to continuous input, incomplete elimination of WWTP and drinking water treatment [13–17].

IBP has been observed to accumulate in the plasma of channel catfish (*Ictalurus punctatus*) [18] and exert irreversible harmful effects on frog embryos [7]. It was also reported IBP could induce liver injury in an adolescent athlete [19]. Furthermore, the ecotoxicity of IBP can be increased considerably when it is present in the mixture with other NSAIDs [20].

These facts have encouraged recent investigation on effective treatment methods to remove IBP in aqueous phase, such as sonication [21,22], ozonation [23], photo-Fenton [24], photolysis [9], heat-activated persulfate [8] and photocatalysis [25]. In the last decade, sulfate radicals ($\text{SO}_4^{\cdot-}$)-based oxidation technologies have attracted increasing interests [26–29]. In this process, $\text{SO}_4^{\cdot-}$ can be generated by activating persulfate or peroxymonosulfate (PMS) with transition metals [30,31], activated carbon [32], UV [33,34], ultrasound [35] and heat [8]. Although Co^{2+} has been proved to be the most effective transition metals for the activation of Oxone [36], the activation of PMS by Fe^{2+} has received increasing interests in recent years since there is always the possibility of adverse health effects caused by Co^{2+} at high concentration. The main drawbacks of Fe^{2+} /Oxone process are the cost of the reagents, in particular Fe(II) [37] and the slow regeneration of Fe(II) [38]. Thus, various methods have been introduced to use cheap Fe(III) salts rather than Fe(II) salts. The way to accelerate the regeneration of Fe(II) is the application of UV irradiation through:



This reaction can not only promote the regeneration of Fe(II) but also produce additional $\cdot\text{OH}$. Furthermore, the use of UV can offer an extra way to generate both $\text{SO}_4^{\cdot-}$ and $\cdot\text{OH}$ through Eq. (2):



H_2O_2 was used as an oxidant in conventional photo-Fenton reaction. Compared with H_2O_2 , Oxone offers some advantages such as the ease of storage and transport, and stability as a solid chemical at ambient temperature. The O—O bond in PMS are cleaved more easily than that in H_2O_2 since the distance of O—O bond in PMS is longer than that in H_2O_2 [39]. In addition, the molar extinction coefficient of PMS at 254 nm is higher than that of H_2O_2 under the same condition [40], indicating PMS is more photosensitive than H_2O_2 .

In this study, we report the degradation of IBP by UV/Fe(III)/PMS process. The UV/Fe(III)/Oxone system has been optimized by varying critical parameters including Fe (III), PMS concentration and solution pH. The influence of inorganic anions has been evaluated on IBP degradation. This contribution also identified the intermediates and products generated during IBP destruction. The possible degradation pathways were proposed.

2. Material and methods

2.1. Reagents

Ibuprofen, Oxone and $\text{Fe}_2(\text{SO}_4)_3 \cdot 9\text{H}_2\text{O}$ were purchased from Sigma-Aldrich while 1,10-phenanthroline was obtained from International Laboratory. *p*-Isobutylbenzaldehyde was purchased from Tokyo Chemical Industry. The salts supplying anions in this study including NaCl, Na_2SO_4 and NaH_2PO_4 were obtained from BDH. All chemicals are in analytic purity and all solvents are HPLC grade and used without further purification. All aqueous solutions were prepared in distilled and deionized water (DDW) with a resistivity of 18.0 M Ω from a Millipore Waters Milli-Q water

purification system. Sulfuric acid and sodium hydroxide were used to adjust the initial pH of the solutions.

2.2. Procedures and analysis

The photodegradation reaction of CBZ was conducted in a photochemical reactor with a cooling fan to control temperature. Two low-pressure mercury UV lamps emitting monochromatic light at 254 nm were installed in the reactor as the irradiation source. The diagram of the experimental installation is shown in Fig. 1. The surface irradiance was determined to be 2.74×10^{-7} Einsteins $\text{L}^{-1} \text{s}^{-1}$ by iodide–iodate actinometry [41]; The optical path length is determined to be 10.16 ± 0.04 cm by measuring the photolysis rate of H_2O_2 [42].

The Fe(III) and PMS solutions were freshly prepared before each test. For each test, a desired amount of Fe^{3+} was added into the IBP solution. The reaction was initiated after the addition of an appropriate amount of PMS and simultaneously switching on the UV lamps. The volume of initial reaction solution was fixed at 200 mL in a 300 mL cylindrical borosilicate glass vessel and stirred mechanically in order to ensure thorough mixing during the reaction. Samples were withdrawn at the predetermined time intervals and quenched using excessive sodium nitrite. All the tests were duplicated and the error was below 5%.

The remaining IBP after reaction was determined by HPLC, which was comprised of a Yilite P230 HPLC pump, a Yilite UV 230⁺ UV/vis detector and a RESTEK C18 column (pinnacle DB, 250×4.6 mm, and 5 μm particle size). The maximum adsorption wavelength (λ_{max}) was selected as 210 nm for IBP. An isocratic flow of acetonitrile/0.1% acetic acid (60/40) was used as the mobile phase running at a flow rate of 1.2 mL/min. The concentration of Fe^{2+} was determined colorimetrically using an UV–vis spectrophotometer at 510 nm after adding 1,10-phenanthroline to form a colored complex of Fe^{2+} –phenanthroline.

The identification of intermediates was carried out at an initial IBP concentration of 0.2 mM. The identification of intermediates was performed by a UPLC/ESI-MS system equipped with Bruker amaZon SL ion trap mass analyzer and Dionex UltiMate 3000 Ultra-high Performance Liquid Chromatography (UPLC). The Thermo Hypersil GOLD column (1.9 μm , 50×2.1 mm) was used for UPLC. A gradient method with a flow rate of 0.2 mL/min was used with a mobile phase containing A (5 mM ammonium acetate at pH 4.6) and B (100% acetonitrile). Component A was maintained at 85% during the first 2 min, then B was steadily increased from

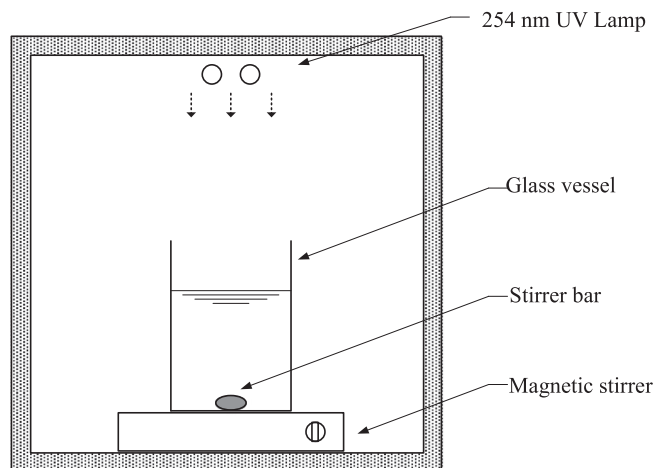


Fig. 1. The diagram of the experimental setup.

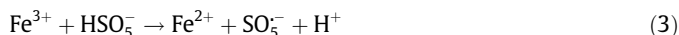
15% to 85% in the next 28 min. Finally, the mobile phase returned to the initial composition until the end of the run.

The reaction intermediates were also identified by SPME (Solid phase microextraction)/GC/MS. SPME analyses were performed using a PAL Combi-xt autosampler (CTC, Switzerland). A 65 μm polydimethylsiloxane/divinylbenzene (PDMS/DVB) SPME fiber (Supelco, Seelze, Germany) was exposed directly into the liquid sample. The aqueous solution was agitated in the incubator (incubation time 1 min, temperature 40 $^{\circ}\text{C}$) at a speed of 250 rpm. The agitator on and off times were 60 and 1 s, respectively. After extraction, the compounds were thermally desorbed for 300 s in the GC injector. After desorption, the fiber was reconditioned in an externally heated needle heater under a light helium flow at a temperature of 270 $^{\circ}\text{C}$. The GC system (TRACE GC ULTRA, Thermo SCIENTIFIC) was equipped with a 30 m HP-5MS capillary column (Agilent Technologies, Santa Clara, US) with an i.d. of 250 μm and a film thickness of 0.25 μm . Helium 5.0 served as the carrier gas. The GC oven temperature program was as follows: initial temperature 50 $^{\circ}\text{C}$ for 2 min, followed by heating at 10 $^{\circ}\text{C min}^{-1}$ to 250 $^{\circ}\text{C}$ and held at 250 $^{\circ}\text{C}$ for 1 min, then at 5 $^{\circ}\text{C min}^{-1}$ from 250 to 280 $^{\circ}\text{C}$, and finally held for 1 min at 280 $^{\circ}\text{C}$. Thermo SCIENTIFIC ISQ MS was run at EI mode. MS transfer line and ion source temperature were set at 300 $^{\circ}\text{C}$ and 250 $^{\circ}\text{C}$, respectively.

3. Results and discussion

3.1. IBP degradation under different conditions

The investigation on IBP degradation under different conditions was conducted. As indicated in Fig. 2, IBP photo-degradation was not observed under the irradiation of UV lamps at 254 nm, which was also reported in previous studies [24]. In the coexistence of Fe^{3+} and Oxone, peroxymonosulfate radicals ($\text{SO}_5^{\cdot-}$) can be generated as shown in Eq. (3):



As a result, around 0.070 mM of Fe (II) was detected after 5 min of reaction in Fe^{3+} /Oxone system (See Fig. 2b). The redox potentials of the reaction (3) solution were measured as indicated in Fig. S2. The addition of Oxone led to the increase of the redox potential. Fig. S2 also shows the redox potentials of reaction (3) solution are lower than that of the solution containing IBP and Oxone, which is due to the consumption of Oxone and the transformation of Fe^{3+} to Fe^{2+} . In previous studies, the formation of ferryl-ion (FeO^{2+}) was reported both in traditional Fenton reaction [43,44] and $\text{Fe}^{2+}/\text{O}_3$ system [45,46]. Fig. S3 shows the absorption spectra of Fe^{3+} , Fe^{2+} , Oxone and Fe^{3+} /Oxone solutions. It is known that FeO^{2+} exhibits strong absorption at the wavelength of 320 nm [45]. As indicated in Fig. S3, the absorption of Oxone and Fe^{2+} at 320 nm is also weak. According to Eq. (1), some Fe^{3+} ions were transformed to Fe^{2+} ions in Fe^{3+} /Oxone system. The absorption of Fe^{3+} /Oxone solution, thus was expected to be weaker than that of Fe^{3+} solution. However, the absorbance of Fe^{3+} /Oxone solution (0.571) is higher than that of Fe^{3+} solution (0.475) at the wavelength of 320 nm, which may indicate the generation of FeO^{2+} in Fe^{3+} /Oxone system. IBP removal efficiency was nearly 50% after 5 min of reaction in Fe^{3+} /Oxone system. However, IBP removal may be mainly attributed to the formation of complex between Fe^{3+} and IBP since no intermediates were identified in this process. As also shown in Fig. 2a, around 70% of removal efficiency was achieved after 30 min of reaction in UV/ Fe^{3+} system. It is well known that the hydrolysis of Fe^{3+} leads to the generation of different Fe^{3+} species, such as $[\text{FeOH}]^{2+}$, $[\text{Fe}(\text{OH})_2]^+$, $[\text{Fe}_2(\text{OH})_2]^{4+}$ and $\text{Fe}(\text{OH})_3$. The most important species is $[\text{FeOH}]^{2+}$ due to its relatively high absorption coefficient for UV light [47]. Under the

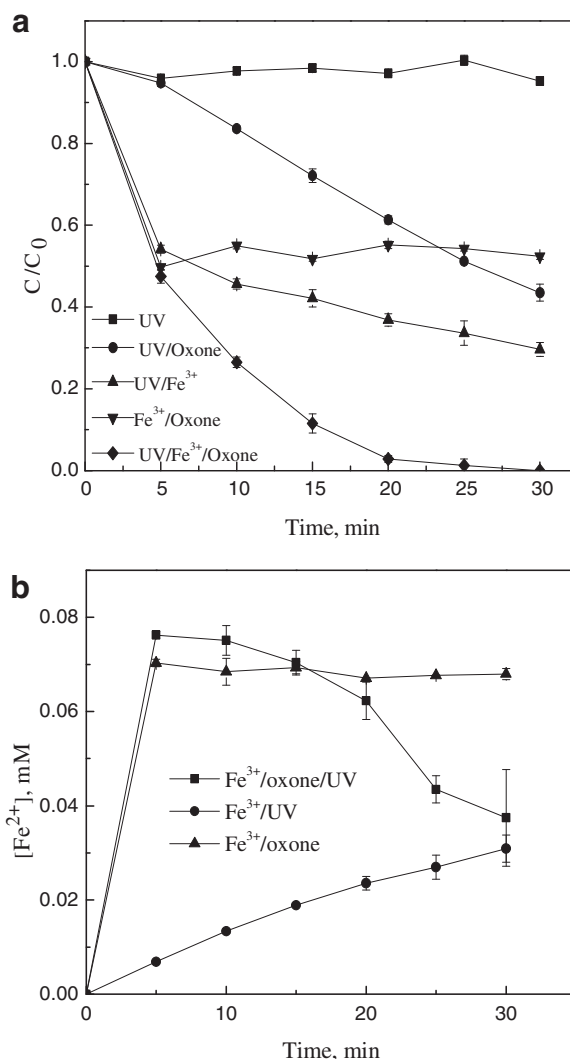
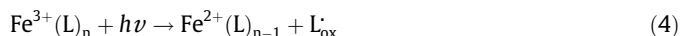


Fig. 2. (a) IBP degradation under different reaction conditions (b) Time course of Fe^{2+} concentration under different reaction conditions (Notes: $[\text{IBP}]_0 = 0.1 \text{ mM}$, $[\text{Fe}^{3+}]_0 = 0.2 \text{ mM}$, $[\text{Oxone}]_0 = 0.2 \text{ mM}$, initial pH is 3.0).

irradiation of UV, the photo reduction of $[\text{FeOH}]^{2+}$ produces hydroxyl radicals (See Eq. (1)) which are partially responsible for the IBP degradation in UV/ Fe^{3+} system.

In addition, Fe^{3+} forms complex with IBP through the carboxylic acid moiety. The ligand-to-metal-charge-transfer reduction of the metal center promotes decarboxylation of IBP as shown in Eq. (4) [48] and further oxidation of decarboxylated intermediates is also driven by hydroxyl radicals in Fe^{3+} /UV system. Reaction 3 is believed to play a significant role in IBP decomposition in Fe^{3+} /UV system since around 60% of IBP molecules forms complex with Fe^{3+} in the reaction solution at pH 3.0 (See Fig. 3c).



It should be noted that Fe^{3+} may also forms complex with the intermediates containing carboxyl group, which may influence the formation of complex between Fe^{3+} and IBP. Thus, IBP degradation may be inhibited.

Around 56% of IBP was eliminated after 30 min in UV/Oxone system. Both hydroxyl radicals and sulfate radicals can be generated in UV/Oxone system as shown in Eq. (2).

The rapid degradation of IBP was found in UV/ Fe^{3+} /Oxone system, where IBP was not detected after 30 min. In this system,

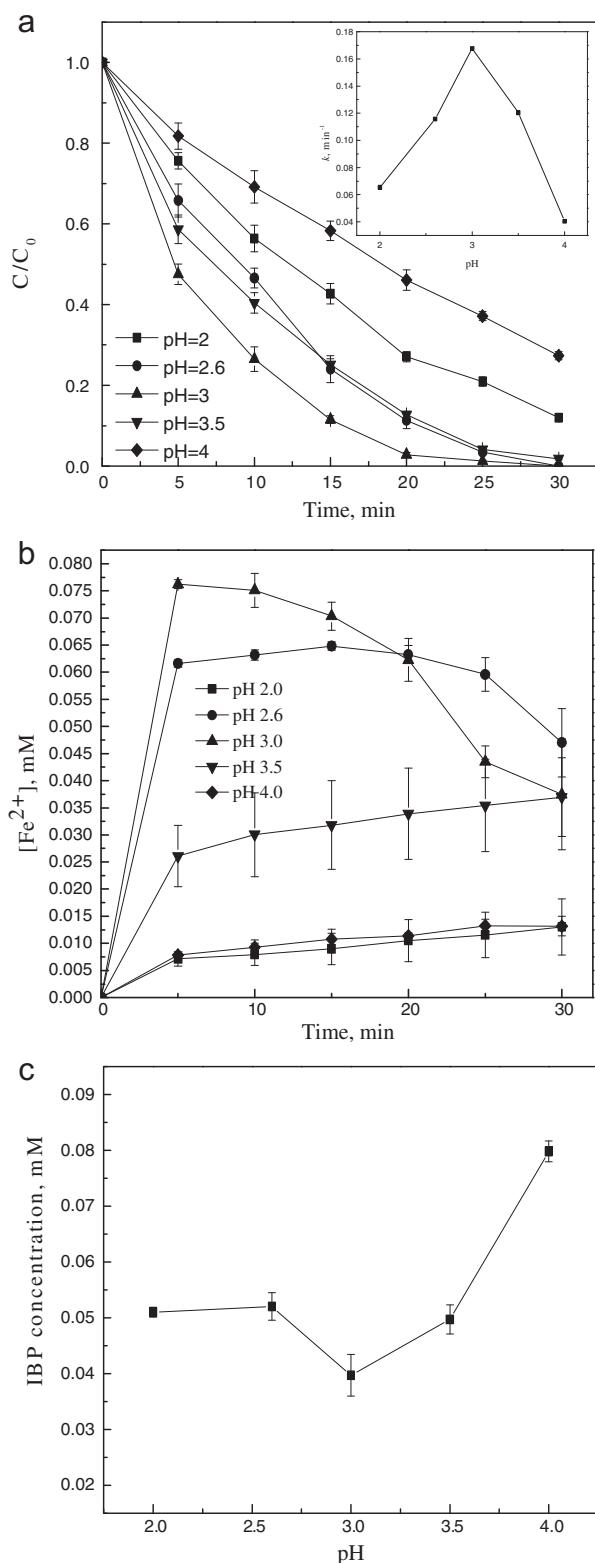
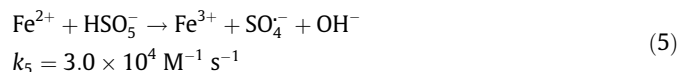


Fig. 3. (a) Effect of initial pH levels on IBP degradation (b) Time course of Fe^{2+} concentration at different pH levels (c) IBP concentration with the presence of 0.2 mM Fe^{3+} at different pH levels (Notes: $[IBP]_0 = 0.1$ mM, $[Fe^{3+}]_0 = 0.2$ mM, $[Oxone]_0 = 0.2$ mM).



The hydroxyl radicals generated by reaction 1 are believed to play an important role in IBP degradation. Reactions 2 and 4 are also believed to be involved in this system.

It should also be noted that UV radiation promotes the oxidation of Fe(II) ions to Fe(III) ions in the presence of dissolved oxygen. Thus, the influence of the presence of dissolved oxygen has been also examined on IBP degradation. As demonstrated in Fig. S4, both purging nitrogen gas and oxygen gas accelerated IBP degradation by UV/ Fe^{3+} and UV/ Fe^{3+} /Oxone processes, suggesting dissolved oxygen may not play a significant role in IBP degradation. The promoting effects of nitrogen gas and oxygen gas may be because they improved the mass transfer in these two systems.

3.2. Effect of pH levels on IBP degradation by UV/ Fe^{3+} /Oxone process

The effects of initial pH levels ranging from 2.00 to 4.00 on IBP degradation were evaluated in this study. IBP degradation was found to follow pseudo first-order kinetics at different pH levels and the observed rate constants are summarized in Fig. 3a. As demonstrated in Fig. 3a, the pH levels played a significant role in IBP degradation and an optimal pH was observed at 3 (See the inset of Fig. 3a). In strongly acidic solution, Fe^{3+} exists as the hexaaquo ion, $Fe(H_2O)_6^{3+}$. As pH increases, Fe^{3+} suffers extensive hydrolysis, leading to the generation of various ferric oxyhydroxides such as $[FeOH]^{2+}$, $[Fe(OH)_2]^+$ and $[Fe_2(OH)_2]^{4+}$ [50], among which photo reduction of $[FeOH]^{2+}$ produces hydroxyl radicals and ferrous ions under the irradiation of UV. The concentration of $[FeOH]^{2+}$ is the highest at pH around 3 [50], resulting in the generation of most hydroxyl radicals and ferrous ions at the initial 20 min (See Fig. 3b). The concentration of free IBP was determined at different pH levels with the presence of Fe^{3+} as demonstrated in Fig. 3c. The highest percent of IBP was found to exist in the form of $Fe^{3+}(L)_n$ at pH 3.0, also leading to the rapidest degradation of IBP through reaction 3. At pH 2.0, 80% of Fe^{3+} exists as Fe^{3+} while 20% of Fe^{3+} exists as $[FeOH]^{2+}$ [50]. Less $[FeOH]^{2+}$ in the solution generates less hydroxyl radicals and Ferrous ions as shown in Fig. 3b. HSO_5^- can be activated by Fe^{3+} to generate $SO_5^{\cdot-}$ which a weak oxidant. At pH 4.0, the formation of precipitation was observed, suggesting less soluble iron species recycled in the system. The concentration of $[FeOH]^{2+}$ and $Fe^{3+}(IBP)_n$ is also low at pH 4.0. Additionally, the precipitated species are considerably less reactive towards Oxone. All these effects result in the retardation of IBP degradation at pH 4.0.

3.3. Effect of Oxone concentration

Oxone concentration is a critical parameter as the source of sulfate radicals and hydroxyl radicals in UV/ Fe^{3+} /Oxone system. The influence of Oxone dosage on IBP degradation was evaluated by varying $[Oxone]/[Fe^{3+}]$ ratios from 1:4 to 2:1 with Fe^{3+} concentration fixed at 0.2 mM. As indicated in Fig. 4a, the increase of IBP decay rate was observed at the elevation of Oxone concentration when $[Oxone]/[Fe^{3+}]$ ratio was below 1:1. However, the further increase of Oxone concentration failed to accelerate IBP degradation. The enhancement of Oxone concentration might lead to the generation of more sulfate radicals and hydroxyl radicals from the photolysis of Oxone under the irradiation of 254 nm. On the other side, the increase of Oxone concentration also resulted in the production of more Fe^{2+} as shown in Fig. 4b. Thus, Fe^{2+} can act as a scavenger of hydroxyl radicals and sulfate radicals at its high concentration through Eqs. (6) and (7), which have much higher reaction rate constants than that of Eq. (5). Furthermore,

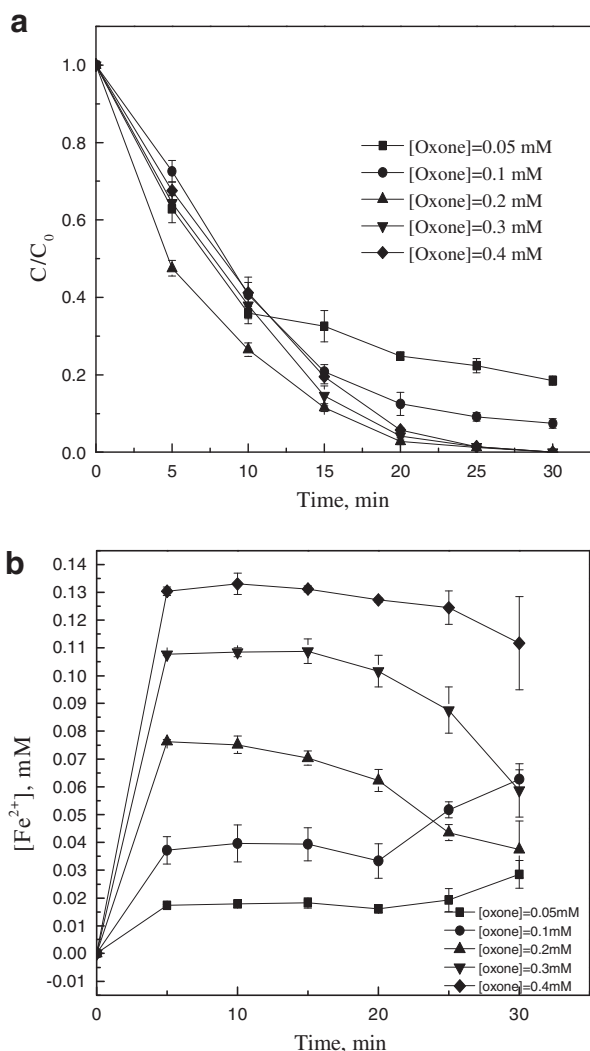
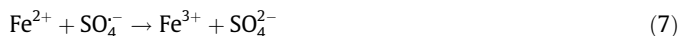


Fig. 4. (a) Effect of Oxone concentration on IBP degradation (b) Time course of Fe^{2+} concentration at different $[\text{Oxone}]_0$ (Notes: $[\text{IBP}]_0 = 0.1 \text{ mM}$, $[\text{Fe}^{3+}]_0 = 0.2 \text{ mM}$, initial pH is 3.0).

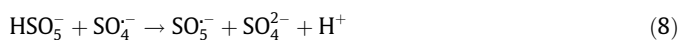
HSO_5^- can also compete for generated sulfate radicals with IBP through Eq. (8) with the high concentration of Oxone [51,36,49].



$$k_6 = 3.0 \times 10^8 \text{ M}^{-1} \text{ s}^{-1}$$



$$k_7 = 3.0 \times 10^8 \text{ M}^{-1} \text{ s}^{-1}$$



$$k_8 < 1 \times 10^5 \text{ M}^{-1} \text{ s}^{-1}$$

3.4. Effect of Fe(III) concentration

The influence of $[\text{Fe}^{3+}]$ ranging from 0.05 to 0.4 mM on IBP degradation has been also investigated with the concentration of Oxone fixed at 0.2 mM. As illustrated in the inset of Fig. 5a, the increase of $[\text{Fe}^{3+}]$ significantly accelerated IBP degradation when $[\text{Fe}^{3+}]$ ratio was below 0.2 mM while IBP decay was retarded with $[\text{Fe}^{3+}]$ above 0.2 mM. When $[\text{Fe}^{3+}]$ was below 0.2 mM, the

enhancement of $[\text{Fe}^{3+}]$ produced more $[\text{FeOH}]^{2+}$ and $\text{Fe}^{3+}(\text{IBP})_n$, leading to the generation of more hydroxyl radicals and Fe^{2+} (See Fig. 5b) as well as the rapid decarboxylation of IBP under the irradiation of UV light. When $[\text{Fe}^{3+}]$ was above 0.2 mM, Fe^{2+} of high concentration might exist in the reaction solution due to the photoreduction of $[\text{FeOH}]^{2+}$ and $\text{Fe}^{3+}(\text{IBP})_n$, where around 0.09 mM Fe^{2+} was detected after 5 min with the initial concentration of Fe^{3+} at 0.3 mM. Fe^{2+} may compete for hydroxyl radicals and sulfate radicals with IBP at its high concentration through Eqs (6) and (7). Furthermore, the presence of Fe^{3+} at high concentration led to less free IBP molecules available in the solution, which may inhibit the degradation of IBP. It is interesting to note that the increase of Fe^{3+} concentration from 0.3 to 0.4 mM failed to generate more Fe^{2+} (See Fig. 5b). It is because part of Fe^{3+} exist in the precipitate of $\text{Fe}(\text{OH})_3$ when $[\text{Fe}^{3+}]$ is 0.4 mM.

3.5. Effect of various inorganic anions

IBP may co-exist with various inorganic ions in various waters. It has been reported that the co-existence of some inorganic anions affects the degradation of organic compounds in the hydroxyl radicals-based and sulfate radicals-based advanced oxidation processes in previous studies which found different results

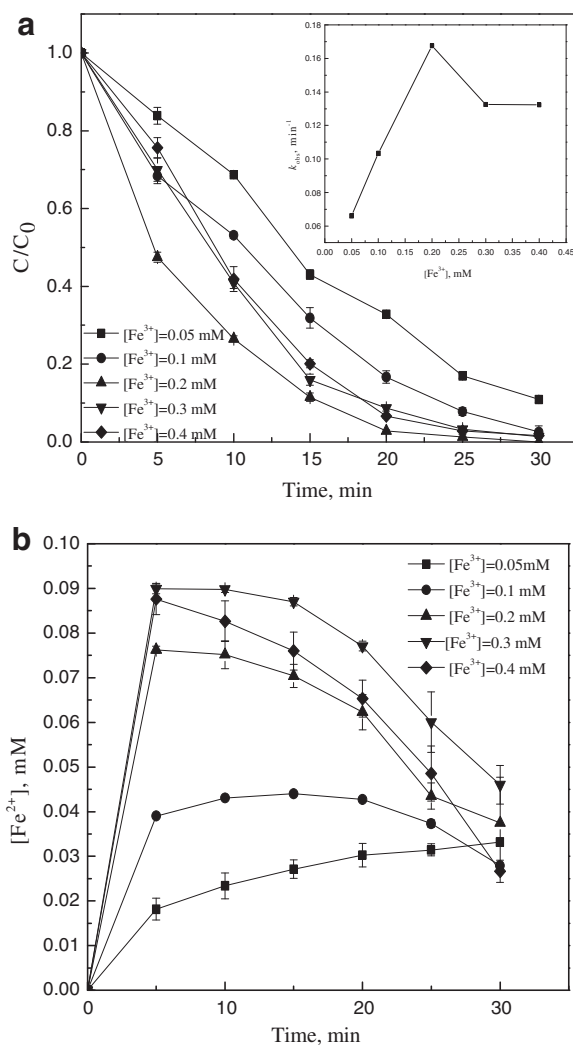


Fig. 5. (a) Effect of Fe^{3+} concentration on IBP degradation (b) Time course of Fe^{2+} concentration at different $[\text{Fe}^{3+}]_0$ (Notes: $[\text{IBP}]_0 = 0.1 \text{ mM}$, $[\text{Oxone}]_0 = 0.2 \text{ mM}$, initial pH is 3.0).

[31,26,52,53]. It was observed SO_4^{2-} , NO_3^- and H_2PO_4^- inhibited the degradation of carbamazepine in the ascending order of $\text{NO}_3^- < \text{SO}_4^{2-} < \text{H}_2\text{PO}_4^-$ while Cl^- dramatically accelerated carbamazepine decay by $\text{Fe}^{2+}/\text{S}_2\text{O}_8^{2-}$ process in our previous study [31]. Wang and Chu also reported SO_4^{2-} significantly retarded the degradation of Rhodamine B (RhB) while Cl^- played a positive role in RhB degradation in $\text{Fe}^{2+}/\text{Oxone}$ system [54]. However, Yang et al. observed Cl^- significantly inhibited the degradation of benzoic acid (BA) and cyclohexanecarboxylic acid (CAA) while Cl^- exerted no obvious influence on the removal of 3-cyclohexene-1-carboxylic acid (3CCA) in $\text{UV}/\text{H}_2\text{O}_2$ and $\text{UV}/\text{S}_2\text{O}_8^{2-}$ systems [53]. This work evaluated the influence of four inorganic anions, including Cl^- , NO_3^- , SO_4^{2-} and H_2PO_4^- on IBP decay by $\text{UV}/\text{Fe}^{3+}/\text{Oxone}$ process.

Fig. 6a shows the addition of 10 mM NO_3^- slightly accelerated IBP degradation while the presence of other anions retarded IBP removal rate, H_2PO_4^- ions exhibiting the most significant inhibiting effects. In order to examine the role of these four anions in IBP degradation by $\text{UV}/\text{Fe}^{3+}/\text{Oxone}$ process, the effects of Cl^- , NO_3^- , SO_4^{2-} and H_2PO_4^- on IBP decay by UV/Fe^{3+} and UV/Oxone processes have also been investigated. Fig. 6b shows the presence of 10 mM Cl^- slightly inhibited IBP degradation as well as NO_3^- and SO_4^{2-} could not affect IBP removal efficiency. As also illustrated in Fig. 6b, IBP degradation was completely inhibited in the presence of 10 mM H_2PO_4^- by UV/Fe^{3+} process. Slight decrease in IBP decay rate was also observed in the presence of 10 mM Cl^- and the presence of 10 mM NO_3^- slightly promoted IBP degradation while SO_4^{2-} and H_2PO_4^- exerts no obvious influence on IBP degradation by UV/Oxone process (See Fig. 6c). The photolysis of NO_3^- generates hydroxyl radicals and other radicals under the irradiation of UV light [55], which may rationalize the promoting effect of NO_3^- on IBP decomposition. It was observed around 27.8% of IBP removal efficiency was achieved in sole-UV system with the presence of 10 mM NO_3^- (Fig. S5). However, the addition of 10 mM NO_3^- failed to increase IBP removal efficiency by 27.8% in $\text{UV}/\text{Fe}^{3+}/\text{Oxone}$ (around 9% increase), UV/Fe^{3+} and UV/Oxone systems (around 15% increase). It is because NO_3^- anions could absorb photons, leading to light attenuation which may partly offset the promoting effect of the radicals generated during the photolysis of NO_3^- . That H_2PO_4^- ions significantly inhibited IBP degradation by $\text{UV}/\text{Fe}^{3+}/\text{Oxone}$ may be because phosphate ions can act as a weak quencher for hydroxyl radicals [56] and the solubility of $\text{Fe}(\text{H}_2\text{PO}_4)_3$ is very low, leading to the generation of precipitate with the addition of H_2PO_4^- ions. As demonstrated in Fig. 6c, H_2PO_4^- ions exerted no influence on IBP decay by UV/Oxone process, suggesting the role of H_2PO_4^- ions is insignificant as a radical quencher. Fig. 6b shows no IBP degradation was observed in the coexistence of 10 mM H_2PO_4^- ions in UV/Fe^{3+} system, indicating around 35% removal of IBP in $\text{UV}/\text{Fe}^{3+}/\text{Oxone}$ system with the addition of 10 mM H_2PO_4^- was attributed to UV/Oxone process. It is interesting to note 56.5% of IBP removal efficiency, which is much higher than IBP removal efficiency (around 35%) in $\text{UV}/\text{Fe}^{3+}/\text{Oxone}$ system with the addition of 10 mM H_2PO_4^- , can be achieved in UV/Oxone system without the addition of anions. This is because the generation of precipitate retarded the penetration of UV light. The inhibiting effect of SO_4^{2-} ions in $\text{UV}/\text{Fe}^{3+}/\text{Oxone}$ system may be because SO_4^{2-} can reduce half-reaction reduction potential of sulfate radical ($E^\circ_{(\text{SO}_4^{\cdot-}/\text{SO}_4^{2-})}$) theoretically [54] since SO_4^{2-} ions showed no effect on IBP degradation in UV/Fe^{3+} system.

In the presence of 10 mM Cl^- , the pseudo-first-order reaction rate constant of IBP degradation was reduced by 27% for $\text{UV}/\text{Fe}^{3+}/\text{Oxone}$, 12.9% for UV/Fe^{3+} and 24% for UV/Oxone , respectively. In our previous study, the presence of 1 mM Cl^- ions significantly accelerated the degradation of carbamazepine by $\text{Fe}^{2+}/\text{S}_2\text{O}_8^{2-}$ process and the higher Cl^- concentration, the faster carbamazepine degradation. Anipsitakis et al. also saw the increase of

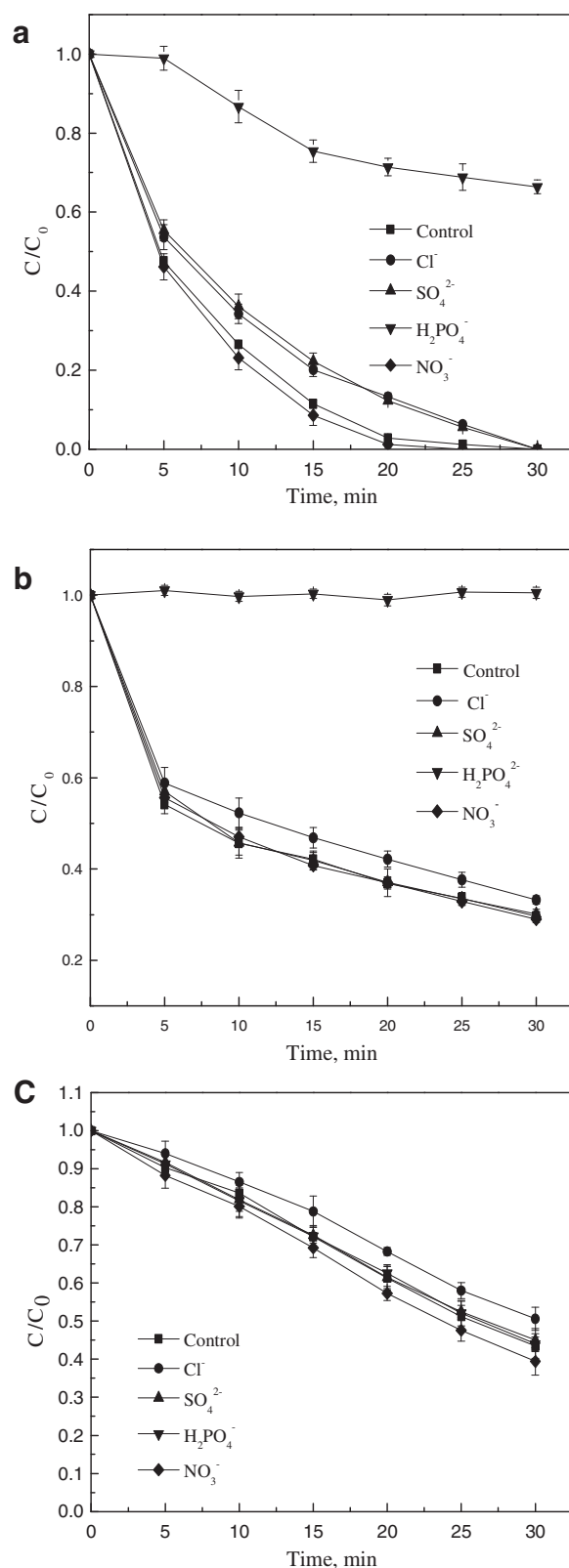
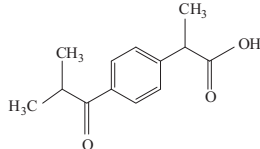
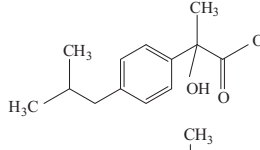
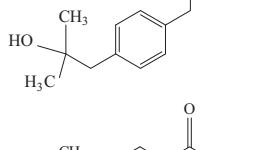
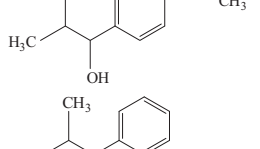
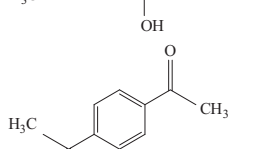
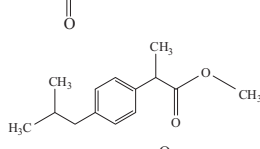
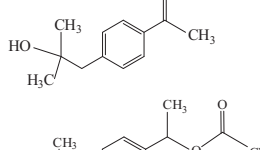
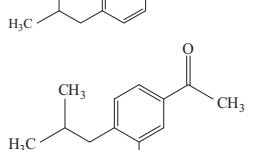
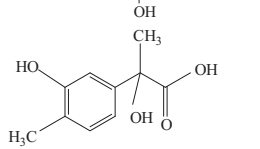
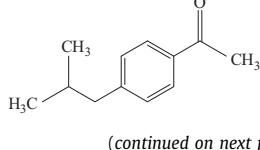




Fig. 6. (a) Effect of inorganic anions on IBP degradation by $\text{UV}/\text{Fe}^{3+}/\text{Oxone}$ process (b) Effect of inorganic anions on IBP degradation by UV/Fe^{3+} process (c) Effect of inorganic anions on IBP degradation by UV/Oxone process (Notes: $[\text{IBP}]_0 = 0.1$ mM, $[\text{Fe}^{3+}]_0 = 0.2$ mM, $[\text{Oxone}]_0 = 0.2$ mM, initial pH is 3.0).

phenol degradation rate in the presence of Cl^- in $\text{Co}^{2+}/\text{Oxone}$ system [26]. It is known chloride ion can act as an important OH and $\text{SO}_4^{\cdot-}$ scavenger, leading to the generation of Cl^\cdot (Eqs. (9)–(11)).

Table 1

Intermediates and products detected by LC–MS/MS and SPME/GC/MS during IBP degradation by UV/Fe³⁺/Oxone process (Note: the intermediate marked with * is identified by NIST library match).

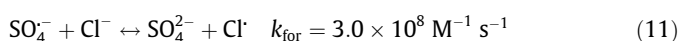
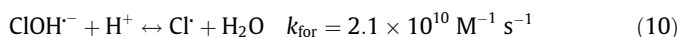
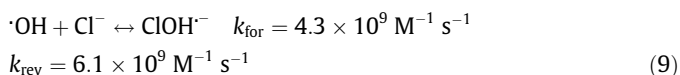
| Product ID | Retention time | El/MS m/z | Proposed structure |
|------------|----------------|--------------------------------|---|
| 1 | 17.93 | 219(220), 174, 159, 144 |  |
| 2 | 17.05 | 222, 179, 163, 123 |  |
| 3 | 16.77 | 178 |  |
| 4 | 16.40 | 192, 177, 163, 149, 135 |  |
| 5 | 15.75 | 149(150), 133, 121, 107 |  |
| 6* | 15.08 | 147, 132, 119, 104, 91, 77, 65 |  |
| 7* | 14.52 | 220, 177, 161, 117 |  |
| 8 | 14.37 | 192, 177, 161, 150 |  |
| 9* | 14.29 | 220, 178, 160, 135, 117, 104 |  |
| 10 | 13.97 | 192, 177, 161, 149, 131 |  |
| 11 | 13.87 | 196, 152, 135, 106, 77 |  |
| 12* | 13.31 | 176, 161, 134 |  |

(continued on next page)

Table 1 (continued)

| Product ID | Retention time | EI/MS m/z | Proposed structure |
|------------|----------------|--------------------------------|--------------------|
| 13* | 12.88 | 178, 163 | |
| 14* | 11.98 | 148, 133, 105, 77, 51 | |
| 15* | 11.78 | 162, 120, 91, 77 | |
| 16* | 11.67 | 150, 133, 119, 107, 99, 77 | |
| 17 | 10.75 | 166, 151, 123, 95, 81 | |
| 18* | 10.52 | 160, 117, 104, 91, 77, 65 | |
| 19* | 9.9 | 162, 133, 339, 105, 91, 77, 65 | |

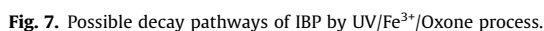
The molecular structure of carbamazepine contains an olefinic double bond which is susceptible to the attack of chlorine radicals. Reaction rate constants for Cl^\cdot with olefins have been reported to be about 3 orders of magnitude higher than that for Cl^\cdot with aromatic or alkane analogues [57], which justifies the accelerating effect of Cl^\cdot ions on the degradation of carbamazepine. For the case of phenol, -OH group on the benzene ring is electron-donating group, which makes the ortho- and para-positions subject to the attack of chlorine radicals. The reaction rate constant for Cl^\cdot with phenol was reported to be $2.5 \times 10^5 \text{ M}^{-1} \text{ s}^{-1}$ [57]. In this work, there are two side chains on the benzene ring of IBP: one is isobutyl and the other is propanoic acid. The isobutyl group is electron-donating group and the group of propanoic acid is electron-withdrawing group, suggesting the ortho-position of isobutyl group on the benzene ring susceptible to the attack of chlorine radicals. On the other side, the steric effects of isobutyl group retard the attack of the radicals. Thus, Cl^\cdot and Cl^\cdot may attack the side chains of IBP. Cl^\cdot and Cl^\cdot which more efficiently target the electron-rich compound or group, are less reactive and more selective than OH and $\text{SO}_4^{\cdot-}$. The two side chains of IBP are electron-poor group, indicating the attack of chlorine radicals on the side chains may be also inefficient. As a result, the presence of chloride ions inhibited IBP degradation in these three processes.



3.6. Identification of IBP degradation intermediates and proposed degradation pathways

IBP degradation intermediates by UV/Fe³⁺/Oxone process were identified by UPLC/ESI-MS with the m/z range of 50–500 in negative ionization mode. SPME (Solid phase microextraction)/GC/MS was also used to identify IBP degradation intermediates for the first time. Molecular structures were proposed for each intermediate/product on the basis of the molecular ion masses and MS fragmentation patterns (MS spectra for each intermediate/product provided in the [Supplementary Materials](#)). Only two intermediates (Compound 2 and 4) were identified by UPLC/ESI-MS. All nineteen intermediates were identified by SPME/GC/MS in this study, including some (such as compounds 6, 7, 9, 10, 15 and 17) which escaped from detection in previous studies. Among the intermediates, compounds 6(1,1'-(1,4-phenylene)bis-ethanone), 7(Ibuprofen methyl ester), 9(Benzenemethanol, α -methyl-4-(2-methylpropyl)-,acetate), 12(4'-(2-Methylpropyl)acetophenone), 13(1-(1-hydroxyethyl)-4-isobutyl-benzene), 14(1-(4-ethylphenyl)-ethanone), 15(p-Isobutylbenzaldehyde), 16(4-(2-methylpropyl)-phenol), 18(1-ethenyl-4-(2-methylpropyl)-benzene) and 19(1-ethyl-4-(2-methylpropyl)-benzene) were identified according to NIST library match. Matching information is shown in [Table S1](#). The probability values of compounds 7, 9, 13 and 15 are greater than 90, indicating the match between these four intermediates and the reference compounds is very good. Ibuprofen methyl ester was synthesized according to previous study [58] and the probability value of the synthesized ibuprofen methyl ester is 94.7, suggesting the match between synthesized ibuprofen methyl ester and reference ibuprofen methyl ester in NIST library is very good. Comparison between the retention time and MS spectra of compound 7 and synthesized

Fig. 7 describes the possible reaction pathways for IBP degradation by UV/Fe³⁺/Oxone process. Three primary intermediates (compound 1, 2 and 19) were generated due to the attack of sulfate radicals and hydroxyl radicals on the two side chains of IBP at the first stage. The attack on the side chains is more favorable kinetically than that on the benzene ring, which may explain the lack of detection of ring-hydroxylated IBP intermediates at the initial stage [60]. Compound 1 (oxo-ibuprofen) derives from the attack of hydroxyl radicals or sulfate radicals on the secondary carbon of the isobutyl chain. Compound 2 comes from the hydroxylation of IBP due to the attack on the tertiary carbon of the propanoic acid chain. The decarboxylation of the propanoic acid chain led to the generation of compound 19. These three primary intermediates were detected at low intensity. The demethylation of compound 2 and further hydroxylation on the benzene ring form compound 11. Compound 13 is believed to come from two sources including the hydroxylation of compound 19 due to the attack on the secondary carbon of the ethyl chain and decarboxylation of compound 2, which may justify the detection of compound 13 at high concentration (Fig. S6). The hydroxylation on the tertiary carbon of the isobutyl chain of compound 19 generates compound 3. It is interesting to detect compound 18 which may come from the dehydration of compound 13 in this study, which was also reported during



the oxidative treatment of IBP by KMnO_4 [58] and photocatalytic degradation of IBP [25]. Compound 18 was also detected during IBP phototransformation with the presence of Rose Bengal in previous study [9]. The deprotonation of compound 13 resulted in the production of compound 12 (4-isobutylacetophenone).

In the case of compound 12, the degradation process follows six possible pathways: (1) hydroxylation on the secondary carbon of the isobutyl chain yields compound 4; (2) demethylation of isobutyl chain generates compound 14; (3) hydroxylation on the tertiary carbon of the isobutyl chain resulted in the production of compound 8; (4) decarboxylation produces compound A which was not detected possibly due to its rapid transformation to compound 5 and 16; (5) demethylation of acetyl chain led the generation of compound 15; (6) hydroxylation on the benzene ring to produce compound 10. Compound 8 may also come from the further oxidation of compound 3. Compound 14 can be further oxidized to reach compound 6. Compound 5 and 16 are believed to derive from the hydroxylation on the benzene ring of compound A. Compound 16 can be again hydroxylated to generate compound 17.

It is unexpected to detect two esters (compound 7 and 9) in this study. Compound 9 may come from the esterification reaction between compound 13 and acetic acid. Although acetic acid was not identified in this study, the generation of acetic acid is reasonable theoretically since the decarboxylation of compound 12 can reach compound A and acetaldehyde. Choina et al. reported the detection of acetic acid during IBP degradation by photocatalysis [25]. Compound 7 may derive from the esterification reaction between IBP and methanol.

As indicated in Fig. S6, the major byproducts remained after the complete removal of IBP could be assigned to compounds 6, 12 and 13 with 26.3%, 37.2% and 17.6% of the total intensities, respectively. Although compound 12 (4-isobutylacetophenone) has been proven to be quite toxic [61], the complete degradation of compound 12 is expected since the intensity of compound decreased significantly after 20 min of IBP degradation reaction.

4. Conclusions

The degradation of IBP was investigated by UV/ Fe^{3+} /Oxone process. IBP decay was found to follow pseudo first-order kinetics. Experimental results also show that the performance of UV/ Fe^{3+} /Oxone process was influenced by operating parameters, such as the concentration of Fe^{3+} and Oxone, initial solution pH, and inorganic salts. Optimum IBP removal efficiency was observed at an initial solution pH of 3.0 within the investigated pH range of 2.0–4.0. Optimum molar ratio of Fe^{3+} /Oxone/IBP was identified to be 2:2:1. The presence of certain inorganic anions exerted a significant effect on the UV/ Fe^{3+} /Oxone process. It was found that Cl^- , SO_4^{2-} and H_2PO_4^- demonstrated adverse effects on IBP degradation, among which H_2PO_4^- exhibited the most significant influence in the process. The existence of NO_3^- , however, slightly facilitated the decomposition of IBP. In addition, 19 intermediates were identified during IBP degradation by UV/ Fe^{3+} /Oxone process. The possible decay pathways were proposed accordingly. Decarboxylation and hydroxylation were found to be major reaction mechanisms for IBP degradation in this process.

Acknowledgment

This work was supported by “the Fundamental Research Funds for the Central University, China”. The authors are also grateful to all anonymous reviewers who contribute to improving this work.

Appendix A. Supplementary data

Supplementary data associated with this article can be found, in the online version, at <http://dx.doi.org/10.1016/j.cej.2015.07.057>.

Reference

- [1] R.P. Schwarzenbach, B.I. Escher, K. Fenner, T.B. Hofstetter, C.A. Johnson, U. von Gunten, B. Wehrli, The challenge of micropollutants in aquatic systems, *Science* 313 (2006) 1072–1077.
- [2] C.G. Daughton, T.A. Ternes, Pharmaceuticals and personal care products in the environment: agents of subtle change?, *Environ Health Perspect.* 107 (1999) 907–938.
- [3] N. Lindqvist, T. Tuhkanen, L. Kronberg, Occurrence of acidic pharmaceuticals in raw and treated sewages and in receiving waters, *Water Res.* 39 (2005) 2219–2228.
- [4] A. Daneshvar, J. Svanfelt, L. Kronberg, G.A. Weyhenmeyer, Winter accumulation of acidic pharmaceuticals in a Swedish river, *Environ. Sci. Pollut. Res.* 17 (2010) 908–916.
- [5] A. Daneshvar, J. Svanfelt, L. Kronberg, M. Prevost, G.A. Weyhenmeyer, Seasonal variations in the occurrence and fate of basic and neutral pharmaceuticals in a Swedish river-lake system, *Chemosphere* 80 (2010) 301–309.
- [6] K. Fent, A.A. Weston, D. Caminada, Ecotoxicology of human pharmaceuticals, *Aquat. Toxicol.* 78 (2006) 207 (vol. 76, p. 122).
- [7] S.M. Richards, S.E. Cole, A toxicity and hazard assessment of fourteen pharmaceuticals to *Xenopus laevis* larvae, *Ecotoxicology* 15 (2006) 647–656.
- [8] A. Ghauch, A.M. Tuqan, N. Kibbi, Ibuprofen removal by heated persulfate in aqueous solution: a kinetics study, *Chem. Eng. J.* 197 (2012) 483–492.
- [9] D. Vione, P.R. Maddigapu, E. De Laurentiis, M. Minella, M. Pazzi, V. Maurino, C. Minerio, S. Kouras, C. Richard, Modelling the photochemical fate of ibuprofen in surface waters, *Water Res.* 45 (2011) 6725–6736.
- [10] M.S. de Graaff, N.M. Vieno, K. Kujawa-Roeleveld, G. Zeeman, H. Temmink, C.J.N. Buisman, Fate of hormones and pharmaceuticals during combined anaerobic treatment and nitrogen removal by partial nitrification-anammox in vacuum collected black water, *Water Res.* 45 (2011) 375–383.
- [11] M. Carballa, F. Omil, T. Ternes, J.M. Lema, Fate of pharmaceutical and personal care products (PPCPs) during anaerobic digestion of sewage sludge, *Water Res.* 41 (2007) 2139–2150.
- [12] M.J. Gomez, M.J.M. Bueno, S. Lacorte, A.R. Fernandez-Alba, A. Agüera, Pilot survey monitoring pharmaceuticals and related compounds in a sewage treatment plant located on the Mediterranean coast, *Chemosphere* 66 (2007) 993–1002.
- [13] C.-P. Yu, K.-H. Chu, Occurrence of pharmaceuticals and personal care products along the West Prong Little Pigeon River in east Tennessee, USA, *Chemosphere* 75 (2009) 1281–1286.
- [14] J.L. Zhao, G.G. Ying, Y.S. Liu, F. Chen, J.F. Yang, L. Wang, X.B. Yang, J.L. Stauber, M.S.J. Warne, Occurrence and a screening-level risk assessment of human pharmaceuticals in the pearl river system, South China, *Environ. Toxicol. Chem.* 29 (2010) 1377–1384.
- [15] C. Fernandez, M. Gonzalez-Doncel, J. Pro, G. Carbonell, J.V. Tarazona, Occurrence of pharmaceutically active compounds in surface waters of the Henares-Jarama-Tajo river system (Madrid, Spain) and a potential risk characterization, *Sci. Total Environ.* 408 (2010) 543–551.
- [16] R. Loos, G. Locoro, S. Contini, Occurrence of polar organic contaminants in the dissolved water phase of the Danube River and its major tributaries using SPE-LC-MS2 analysis, *Water Res.* 44 (2010) 2325–2335.
- [17] C. Wang, H. Shi, C.D. Adams, S. Gamagedara, I. Stayton, T. Timmons, Y. Ma, Investigation of pharmaceuticals in Missouri natural and drinking water using high performance liquid chromatography-tandem mass spectrometry, *Water Res.* 45 (2011) 1818–1828.
- [18] G.C. Nallani, P.M. Paulos, L.A. Constantine, B.J. Venables, D.B. Huggett, Bioconcentration of ibuprofen in fathead minnow (*Pimephales promelas*) and channel catfish (*Ictalurus punctatus*), *Chemosphere* 84 (2011) 1371–1377.
- [19] W.E. Bennett Jr., Y.P. Turmelle, R.W. Shepherd, Ibuprofen-induced liver injury in an adolescent athlete, *Clin. Pediatr.* 48 (2009) 84–86.
- [20] M. Cleuvers, Mixture toxicity of the anti-inflammatory drugs diclofenac, ibuprofen, naproxen, and acetylsalicylic acid, *Ecotox. Environ. Safe* 59 (2004) 309–315.
- [21] R. Xiao, Z. He, D. Diaz-Rivera, G.Y. Pee, L.K. Weavers, Sonochemical degradation of ciprofloxacin and ibuprofen in the presence of matrix organic compounds, *Ultrason. Sonochem.* 21 (2014) 428–435.
- [22] F. Mendez-Arriaga, R.A. Torres-Palma, C. Petrier, S. Esplugas, J. Gimenez, C. Pulgarin, Ultrasonic treatment of water contaminated with ibuprofen, *Water Res.* 42 (2008) 4243–4248.
- [23] M.J. Quero-Pastor, M.C. Garrido-Perez, A. Acevedo, J.M. Quiroga, Ozonation of ibuprofen: a degradation and toxicity study, *Sci. Total Environ.* 466 (2014) 957–964.
- [24] F. Mendez-Arriaga, S. Esplugas, J. Gimenez, Degradation of the emerging contaminant ibuprofen in water by photo-Fenton, *Water Res.* 44 (2010) 589–595.
- [25] J. Choina, H. Kosslick, C. Fischer, G.U. Flechsig, L. Frunza, A. Schulz, Photocatalytic decomposition of pharmaceutical ibuprofen pollutions in water over titania catalyst, *Appl. Catal. B-Environ.* 129 (2013) 589–598.

- [26] G.P. Anipsitakis, D.D. Dionysiou, M.A. Gonzalez, Cobalt-mediated activation of peroxymonosulfate and sulfate radical attack on phenolic compounds. Implications of chloride ions, *Environ. Sci. Technol.* 40 (2006) 1000–1007.
- [27] K.H. Chan, W. Chu, Degradation of atrazine by cobalt-mediated activation of peroxymonosulfate: different cobalt counteranions in homogenous process and cobalt oxide catalysts in photolytic heterogeneous process, *Water Res.* 43 (2009) 2513–2521.
- [28] G.A.A. Ghauch, S. Naim, Degradation of sulfamethoxazole by persulfate assisted micrometric Fe^0 in aqueous solution, *Chem. Eng. J.* 228 (2013) 1168–1181.
- [29] M.M. Ahmed, S. Chiron, Solar photo-Fenton like using persulfate for carbamazepine removal from domestic wastewater, *Water Res.* 48 (2014) 229–236.
- [30] G.P. Anipsitakis, D.D. Dionysiou, Degradation of organic contaminants in water with sulfate radicals generated by the conjunction of peroxymonosulfate with cobalt, *Environ. Sci. Technol.* 37 (2003) 4790–4797.
- [31] Y.F. Rao, L. Qu, H.S. Yang, W. Chu, Degradation of carbamazepine by Fe(II) -activated persulfate process, *J. Hazard. Mater.* 268 (2014) 23–32.
- [32] J. Zhang, X. Shao, C. Shi, S. Yang, Decolorization of Acid Orange 7 with peroxymonosulfate oxidation catalyzed by granular activated carbon, *Chem. Eng. J.* 232 (2013) 259–265.
- [33] T.K. Lau, W. Chu, N.J.D. Graham, The aqueous degradation of butylated hydroxyanisole by $\text{UV}/\text{S}_2\text{O}_8^{2-}$: study of reaction mechanisms via dimerization and mineralization, *Environ. Sci. Technol.* 41 (2007) 613–619.
- [34] Y.-H. Guan, J. Ma, X.-C. Li, J.-Y. Fang, L.-W. Chen, Influence of pH on the formation of sulfate and hydroxyl radicals in the $\text{UV}/\text{peroxymonosulfate}$ system, *Environ. Sci. Technol.* 45 (2011) 9308–9314.
- [35] L. Bingzhi, L. Lin, L. Kuangfei, Z. Wei, L. Shuguang, L. Qishi, Removal of 1,1,1-trichloroethane from aqueous solution by a sono-activated persulfate process, *Ultrason. Sonochem.* 20 (2013) 855–863.
- [36] G.P. Anipsitakis, D.D. Dionysiou, Radical generation by the interaction of transition metals with common oxidants, *Environ. Sci. Technol.* 38 (2004) 3705–3712.
- [37] C. Minero, M. Lucchiari, D. Vione, V. Maurino, Fe(III) -enhanced sonochemical degradation of methylene blue in aqueous solution, *Environ. Sci. Technol.* 39 (2005) 8936–8942.
- [38] Y.R. Wang, W. Chu, Photo-assisted degradation of 2,4,5-trichlorophenoxyacetic acid by Fe(II) -catalyzed activation of oxone process: the role of UV irradiation, reaction mechanism and mineralization, *Appl. Catal. B-Environ.* 123 (2012) 151–161.
- [39] J. Flanagan, W.P. Griffith, A.C. Skapski, The active principle of Caro's acid, HSO_5^- : X-ray crystal structure of $\text{KHSO}_5 \cdot \text{H}_2\text{O}$, *J. Chem. Soc. Chem. Commun.* (1984) 1574–1575.
- [40] G.P. Anipsitakis, D.D. Dionysiou, Transition metal/UV-based advanced oxidation technologies for water decontamination, *Appl. Catal. B-Environ.* 54 (2004) 155–163.
- [41] R.O. Rahn, M.I. Stefan, J.R. Bolton, E. Goren, P.S. Shaw, K.R. Lykke, Quantum yield of the iodide-iodate chemical actinometer: dependence on wavelength and concentration, *Photochem. Photobiol.* 78 (2003) 146–152.
- [42] J.H. Baxendale, J.A. Wilson, The photolysis of hydrogen peroxide at high light intensities, *Trans. Faraday Soc.* 53 (1957) 344–356.
- [43] W.C. Bray, M.H. Gorin, Ferryl ion, a compound of tetravalent iron, *J. Am. Chem. Soc.* 54 (1932) 2124–2125.
- [44] B. Ensing, F. Buda, P. Blochl, E.J. Baerends, Chemical involvement of solvent water molecules in elementary steps of the fenton oxidation reaction, *Angew. Chem.-Int. Edit.* 40 (2001) 2893–2895.
- [45] F. Jacobsen, J. Holcman, K. Sehested, Activation parameters of ferryl ion reactions in aqueous acid solutions, *Int. J. Chem. Kinet.* 29 (1997) 17–24.
- [46] O. Pestovsky, A. Bakac, Aqueous ferryl(IV) ion: kinetics of oxygen atom transfer to substrates and oxo exchange with solvent water, *Inorg. Chem.* 45 (2006) 814–820.
- [47] J.J. Pignatello, E. Oliveros, A. MacKay, Advanced oxidation processes for organic contaminant destruction based on the Fenton reaction and related chemistry, *Crit. Rev. Environ. Sci. Technol.* 37 (2007) (2006) 273–275 (vol. 36, p. 1).
- [48] J.J. Pignatello, E. Oliveros, A. MacKay, Advanced oxidation processes for organic contaminant destruction based on the Fenton reaction and related chemistry, *Crit. Rev. Environ. Sci. Technol.* 36 (2006) 1–84.
- [49] C. Brandt, R. Vaneldik, Transition metal-catalyzed oxidation of sulfur(IV) oxides. atmospheric-relevant processes and mechanisms, *Chem. Rev.* 95 (1995) 119–190.
- [50] H. Gallard, J. De Laat, B. Legube, Spectrophotometric study of the formation of iron(III)-hydroperoxy complexes in homogeneous aqueous solutions, *Water Res.* 33 (1999) 2929–2936.
- [51] C. Walling, Fenton's reagent revisited, *Accounts Chem. Res.* 8 (1975) 125–131.
- [52] G.-D. Fang, D.D. Dionysiou, Y. Wang, S.R. Al-Abed, D.-M. Zhou, Sulfate radical-based degradation of polychlorinated biphenyls: effects of chloride ion and reaction kinetics, *J. Hazard. Mater.* 227 (2012) 394–401.
- [53] Y. Yang, J.J. Pignatello, J. Ma, W.A. Mitch, Comparison of halide impacts on the efficiency of contaminant degradation by sulfate and hydroxyl radical-based advanced oxidation processes (AOPs), *Environ. Sci. Technol.* 48 (2014) 2344–2351.
- [54] Y.R. Wang, W. Chu, Degradation of a xanthene dye by Fe(II) -mediated activation of oxone process, *J. Hazard. Mater.* 186 (2011) 1455–1461.
- [55] J. Mack, J.R. Bolton, Photochemistry of nitrite and nitrate in aqueous solution: a review, *J. Photochem. Photobiol. A-Chem.* 128 (1999) 1–13.
- [56] J. Kochany, E. Lipczynskakochany, Application of the EPR spin-trapping technique for the investigation of the reactions of carbonate, bicarbonate, and phosphate anions with hydroxyl radicals generated by the photolysis of H_2O_2 , *Chemosphere* 25 (1992) 1769–1782.
- [57] K. Hasegawa, P. Neta, Rate constants and mechanisms of reaction of Cl_2^- radicals, *J. Phys. Chem.* 82 (1978) 854–857.
- [58] G. Caviglioli, P. Valeria, P. Brunella, C. Sergio, A. Attilia, B. Gaetano, Identification of degradation products of ibuprofen arising from oxidative and thermal treatments, *J. Pharm. Biomed. Anal.* 30 (2002) 499–509.
- [59] R.K. Szabo, C. Megyeri, E. Illes, K. Gajda-Schranz, P. Mazellier, A. Dombi, Phototransformation of ibuprofen and ketoprofen in aqueous solutions, *Chemosphere* 84 (2011) 1658–1663.
- [60] G. Ruggeri, G. Ghigo, V. Maurino, C. Minero, D. Vione, Photochemical transformation of ibuprofen into harmful 4-isobutylacetophenone: pathways, kinetics, and significance for surface waters, *Water Res.* 47 (2013) 6109–6121.
- [61] M.A. Miranda, I. Morera, F. Vargas, M.J. Gomezlechón, J.V. Castell, In vitro assessment of the phototoxicity of antiinflammatory 2-arylpropionic acids, *Toxicol. Vitro* 5 (1991) 451–455.